Chemistry and Physics of Lipids 206 (2017) 1–8

Contents lists available at ScienceDirect

Chemistry and Physics of Lipids

journal homepage: www.elsevier.com/locate/chemphyslip

Effects of hydroxy-xanthones on dipalmitoylphosphatidylcholine lipid bilayers: A theoretical and experimental study

M.B. Sierra[a], L. Alarcón[a], D. Gerbino[b], V.I. Pedroni[a], F.E. Buffo[c], M.A. Morini[a,*]

[a] Laboratorio de Fisicoquímica, INQUISUR, Departamento de Química, Universidad Nacional del Sur (UNS)-CONICET, Av. Alem 1253, 8000 Bahía Blanca, Argentina
[b] Laboratorio de Química Orgánica, INQUISUR, Departamento de Química, Universidad Nacional del Sur (UNS)-CONICET, Av. Alem 1253, 8000 Bahía Blanca, Argentina
[c] Dpto. de Matemática, Universidad Nacional del Sur (UNS), Av. Alem 1253, 8000 Bahía Blanca, Argentina

ARTICLE INFO

Article history:
Received 2 December 2016
Received in revised form 15 May 2017
Accepted 16 May 2017
Available online 19 May 2017

Keywords:
DPPC liposome
Xanthones
Zeta potential
Molecular dynamics simulations
Fluidity

ABSTRACT

Xanthones and derivatives are natural active compounds whose interest has been increased due to its several pharmacological effects. In this work, effects of hydroxy-xanthones on the physicochemical properties of dipalmitoylphosphatidylcholine (DPPC) liposomes have been investigated in terms of lipid bilayer fluidity, by means of molecular dynamics simulations and temperature dependence of zeta potential studies. Experimental results predict, in good agreement with simulations, that xanthones are able to be incorporated into DPPC liposomes with certain localization, fluidizing the bilayer. Both effects, localization and fluidity were found to be dependent of the number of hydroxilic substituents of the xanthone and the lipid phase state.

1. Introduction

Lipids are the major component of cell membrane and the phospholipids are one of the most abundant classes of membrane lipids. The phospholipid membranes serve as a barrier and selectively allow molecules to pass to the interior of the cell. As the cell is the central part of life, the understanding of the functionality of cell wall i.e. lipid bilayer membrane under the influence of foreign material is a major challenge in biology.

Xanthones (9H-xanthen-9-ones) are a special class of oxygenated heterocyclic compounds with important biological activities (Chairungsrilerd et al., 1996; Iinuma et al., 1998; Lin et al., 1996). This family of compounds are structurally typified by the presence of a dibenzo-γ-pirone system differing in the position and nature of the substituents. This molecular diversity provides a wide variety of pharmacological properties; e.g. the xanthone skeleton constitutes the core of an important group of natural and biologically active compounds such as bikaverin (de Koning et al., 1988), and α-mangostin (Matsumoto et al., 2003, 2004) (Fig. 1). Moreover, the biological behavior of xanthones can be controlled by introducing specific substituents in their structure (Dodean et al., 2008; Kolokythas et al., 2002). Plant xanthones are defense compounds against herbivores and microorganisms (Tocci et al., 2011). In humans, xanthones exhibit an array of pharmacological activities, including anti-Alzheimer properties (El-Seedi et al., 2010; Wang et al., 2016, 2012), cardiotonic, antimicrobial and anti-hepatotoxic effects, as well as anti-inflammatory activity.

From the molecular structure shown in Fig. 1, it can be seen that xanthones are hydrophobic compounds which are insoluble in water, but are highly soluble in many organic solvents. Hence, the entrapment of xanthones in liposomes can be of pharmacological advantage, since enhancement of the absorption through the biological membrane by entrapment or solubilization of xanthones in the bilayers of liposomes is anticipated. However, the effect of xanthones on the liposomal state has not been enough clarified. They can also be obtained by synthesis and several strategies to achieve this goal have been described in the literature (Goncalves Azevedo et al., 2012; Menéndez et al., 2014).

The members of the xanthones classes bear different types of substituents that are able to interact with several biological targets exerting different pharmacological activities (Pinto et al., 2005)

* Corresponding author at: Laboratorio de Fisicoquimica, Dpto. De Química, INQUISUR, Universidad Nacional del Sur, Avenida Alem 1253, CP 8000 Bahía Blanca, Pcia. de Buenos Aires, Argentina.
E-mail addresses: mbsierra@uns.edu.ar (M.B. Sierra), lalarcon@uns.edu.ar (L. Alarcón), dgerbino@uns.edu.ar (D. Gerbino), pedroni@criba.edu.ar (V.I. Pedroni), fbuffo@uns.edu.ar (F.E. Buffo), mamorini@criba.edu.ar (M.A. Morini).

http://dx.doi.org/10.1016/j.chemphyslip.2017.05.004
0009-3084/

and hydroxyl is one of the most frequent chemical groups found in natural and synthetic xanthones. Fig. 2 shows the structures of the hydroxylated xanthones studied in this work.

It is reported in the literature that a small perturbation to the bilayer can change the fluidity of the bilayer (Bothun, 2008; Park et al., 2006, 2005). The fluidity in membrane is directly related to the structural arrangement of the lipid molecules. However, this structural arrangement of lipid may differ for adjacent to and far from the foreign material adsorption site. Brittes et al. (2010) reported that added molecules induced decrease of the transition temperature and cooperativity of DPPC bilayers, which can be interpreted as an increasing membrane fluidity effect.

In a previous work from our research group (Morini et al., 2015) it was shown that the surface charge of the liposome mainly depends on the kind of lipid and conditions such as temperature, phase state of the liposome. Temperature dependence Zeta Potential Studies (ZP) were proposed (Sierra et al., 2016) to analyze the thermotropic behavior of mixtures of synthetic phospholipids in unilamellar aqueous suspensions in the presence or absence of ions. Since the lipid phase transition influences the surface potential of the liposome reflecting a sharp ZP change during the phase transition (Tatulian, 1983), we proposed this technique as a screening method for transition temperatures in complex systems given its high sensitivity and small amount of sample required, that is, 70% less than that required in the use of conventional calorimeters. The zeta potential as a function of temperature technique can be used to detect both the main transition and the pretransition of lipids. This method allows the assessment of phase changes in the studied lipid system as well as their surface charge.

In addition to other studies, the analysis of the zeta potential changes with temperature would provide information on the structural arrangement of the lipid in the liposome under study. According to our studies (Morini et al., 2015), DPPC shows negative values of zeta potential in liquid crystalline state and positive ones in solid crystalline state. That behavior was explained in terms of the molecular conformation acquired by DPPC either exposing the phosphate group in the fluid state, or exposing the coline group in the gel state. The reorientation of the head group directors in PC by phase transitions is already known from the literature, especially in the field of ^{31}P – NMR and X-ray diffraction (Hauser et al., 1981; Sulkowski et al., 2005; Tieleman et al., 1997).

The results of the non-invasive zeta potential approach constitute very reliable data because there are no perturbation problems related to invasive techniques.

In this work, we used the temperature dependence of zeta potential for the thermotropic study of the chosen systems. We also performed molecular dynamics simulations to investigate the interaction of different xanthones with DPPC bilayers at the molecular scale. We also aimed at understanding how xanthones affect the dynamics and ordering of the lipids together with their impact on membrane fluidity. We made root mean square deviation (RMSD) calculations (Villarreal et al., 2008). for the lipid molecules, both for xanthone-containing membrane and for a pure lipid bilayer taken as a reference. RMSD calculations measure the deviation of certain atoms, generally heavy atoms, with respect to a reference set of coordinates or initial configuration. Thus, by measuring the time evolution of the RMSD of the lipid atoms we provided a good estimation of membrane fluidity.

To our knowledge, this paper is the first theoretical and experimental study of the interactions of hydroxy-xanthones with model membranes by means of the temperature dependence of the zeta potential and molecular dynamics simulations. The aim of this work was to get information on the basic modifications induced by these dopants on the lipid organization, particularly refered to membrane fluidity and xanthones localization within the membrane. Therefore, the effect of these compounds on the biophysical properties and structure of lipid bilayers are questions that are opened in the present work.

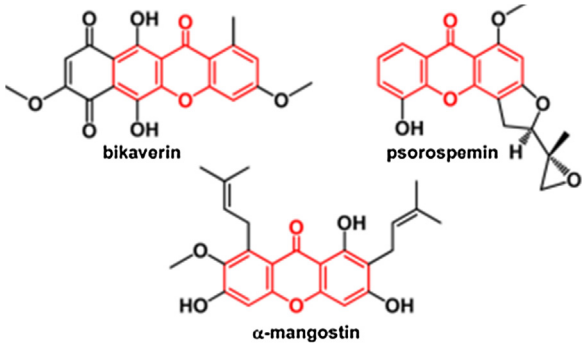

Fig. 1. Some representative natural xanthones.

2. Methodology

2.1. Experimental

2.1.1. Materials

1,2-Dipalmitoyl-*sn*-glycero-3-phosphocholine (DPPC) was obtained from Avanti Polar Lipids Inc. (Alabaster, AL) and used as received. Hydroxy-xanthones were obtained by synthesis, characterized and purified in the synthesis organic laboratory directed by Dr. D.Gerbino (Menéndez et al., 2014; Koh et al., 2015). The following xanthones (XAs) were synthesized: xanthone skeleton (XA); 1-Hydroxyxanthone (XA_1); 1,3-Dihydroxyxanthone($XA_{1,3}$) and 1,3,6-Trihydroxyxanthone($XA_{1,3,6}$). Chloroform and methanol were of analytical grade. Dispersions were prepared with ultrapure water (Super Q Millipore system).

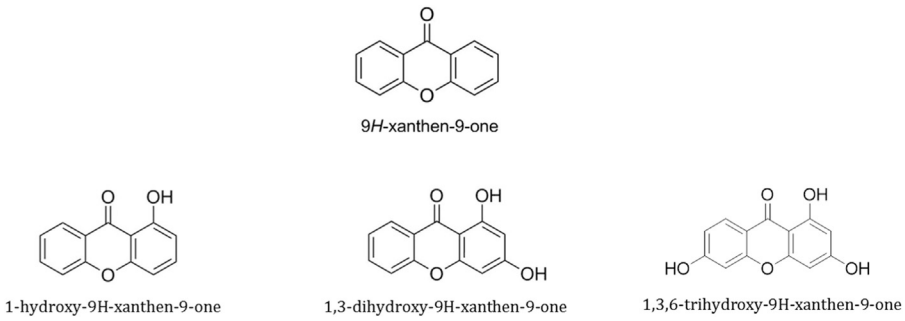

Fig. 2. Structures of the hydroxylated xanthones. xanthone skeleton (XA); 1-Hydroxyxanthone (XA_1); 1,3-Dihydroxyxanthone($XA_{1,3}$) and 1,3,6-Trihydroxyxanthone($XA_{1,3,6}$).

2.1.2. Liposome preparation

Liposomes of DPPC-XAs were prepared weighing appropriate amounts of each one in order to obtain proportions X_{XAs} of 0.3, where X_{XAs} is the mole fraction of xanthones in the mixture of liposomes without considering the solvent. The proportion of dopant was mainly chosen by preliminary unpublished studies carried out in our laboratory and is coincident with bibliography reports (Onuki et al., 2008). In each ZP experiment, for the mole fraction 0.3, on the order of 4 mg of dry DPPC was weighed and then the appropriate weight of dry XAs was added. In each ZP experiment, for the mole fraction 0.3, on the order of 4 mg of dry DPPC was weighed and then the appropriate weight of dry xanthone was added. Mixtures of DPPC-XAs were dissolved in a chloroform-methanol mixture that was removed by evaporation with N_2 stream to obtain a dry lipid film. Remaining solvent was removed keeping the films under high vacuum for additional 2 h in a Thermo Scientific Speed Vac SPD11V. The resulting dry lipid films were then hydrated with 3 mL of water, pH 6.5, and homogenized with cycles of vigorous vortexing at around 10 °C above the transition temperature of the lipid. The final concentration of the dispersions was on the order of 3 mM for each ZP experiment.

This heating-vortexing combination yields a polydispersed population of MLVs. Unilamellar vesicles (LUVs) were obtained by sequential extrusion of the MLVs dispersions in an Avanti Mini-Extruder, through a polycarbonate membrane of 100 nm pore size at around ten degrees centigrade above the transition temperature of the lipid (Mabrey and Sturtevant, 1976; Lasic, 1997; Rodríguez-Pulido et al., 2008a, 2009, 2008b).

The final conductivity of all the dispersions was slightly higher than that of MilliQ water. In the case of pH, no significative differences between the dispersions and MilliQ water were found.

2.1.3. Methods

2.1.3.1. Zeta potential. Zeta potential (ζ), size distribution and conductivity of DPPC and DPPC-XAs liposomes were determined in a Zetasizer Nano ZS90 equipment (Malvern Instruments Ltd., UK). Measurements were performed in the range between 60 °C and 20 °C with successively lowered temperatures, allowing the sample to reach equilibrium between measurements, recording a point every 2 °C with a stabilization period of 10 min at constant temperature before measuring. No hysteresis was observed when controlling the heating process (data not shown). Reported data are the average of four different batches of each sample. The pH was registered at the beginning and the end of every measurement.

2.1.3.2. DSC measurement. Calorimetry was performed using a DSC TA Instruments Q20 differential scanning calorimeter. Liposome samples were placed in airtight capsules for DSC. Calorimetry measurements were performed for each mixture between 20 and 60 °C, at a rate of 0.5 °C per minute. No hysteresis was observed when controlling the cooling process (data not shown). Reported data are the average of three different batches of each sample.

2.1.4. Mathematical treatment

Here is presented a methodology for the treatment of the data of the temperature dependence of the ZP method for determining DPPC-XAs mixtures transition temperatures. A model function to adjust those values according to certain predefined objectives is proposed. Then, using the adjustment function, estimations of the transition temperature and the delimiting temperatures corresponding to the start-point and the end-point of the transition phase of the mixture used in each experiment were done.

A set of experimental data $(T_i, \zeta_i), i = 1, \ldots n$ was considered, with n, number of measurements for DPPC-XAs mixture, T_i temperature and ζ_i zeta potential.

It was necessary to find the m-vector A of free parameters that would give the "best fit" to the model function $f(T, A)$, solving the optimization problem:

$$\min_{A\in\mathbb{R}^{2p+1}} \sum_{i=1}^{n} (\zeta_i - f(T_i, A))^2 \tag{1}$$

being this equation called the least squares solution, because the sum of squares of the differences between the function model and the data is minimized. The least squares criterion for data fitting (Eq. (1)) can be expressed as minimizing the squared Euclidean norm of the residual vector with components

$$r_i = \zeta_i - f(T_i, A)$$

because of the shape of the ζ vs. T sequence, a linear combination of trigonometric functions (harmonic functions) as an adjusting model function is proposed:

$$f(T, A) = A_1 + \sum_{j=1}^{p} A_{2j} sen(\omega_j T) + A_{2j+1} cos(\omega_j T) \tag{2}$$

where $\omega_j = 2\pi_j / T_n$ and p is a natural number selected according to the shape of the curve and being A, a free parameter vector of dimension $m = 2p + 1$. The values of p in this kind of adjust oscillate between 3 and 5.

The main transition temperature of the DPPC-XAs mixtures, $T_{transition}$, is the abscissa of the inflection point of $f(T, A_*)$ and is estimated solving the non-linear equation $f''(T, A_*) = 0$ with the Newton method, being A_* the solution of the optimization problem (Eq. (1)).

The strategy to estimate the temperatures corresponding to the start-point and the end-point of the phase transition is to identify the "sudden" change of curvature of the $f(T, A_*)$; the curvature function is calculated by:

$$Cv(T) = \frac{f''(T, A_*)}{\left(\sqrt{1 + f'(T, A_*)^2}\right)^3} \tag{3}$$

2.2. Molecular dynamics simulations

DPPC – XAs membranes were simulated by means of AMBER12 software package, using Lipid11 (Skjevik et al., 2012) force field, choosing a cut off of 10 Å. The bilayer was composed of 128 DPPC molecules (64 per monolayer in an 8 × 8 arrangement), where nine DPPC molecules located at alternate positions in the monolayer were replaced by xanthone molecules, XA_1 in one case and $XA_{1,3,6}$ in the other. Each DPPC-XA membrane was solvated with TIP3P water molecules along the Z axis, assuring a fully hydrated system, and was subjected to periodic boundary conditions along the (X,Y) plane.

Once the system was assembled and hydrated the minimization process was carried out in two steps, both at constant volume. In the first step the solvent was minimized, keeping the membrane fixed, and then released it and minimized the entire system. Then, the system temperature was stabilized using the Langevin thermostat at 323 K for the liquid crystalline state and at 293 K for the solid crystalline state.

A run of 100 ns was then carried out in order to equilibrate the xanthone positions into the bilayer. The distances between neighboring lipids were consistent with experimental values for pure membranes.

The final production data correspond to the last 10ns of the total run and these results are shown in the corresponding figures.

Both equilibration and final production data used a NPT assembly (constant number of atoms N, pressure P and temperature T) with SHAKE activated for bonds with hydrogen.

3. Results

We obtained values of ZP with continuous cooling of DPPC and DPPC-XAs. The results are shown in Fig. 3. The different mixtures of DPPC-XAs with water as solvent exhibited surface charge. This result is similar to that obtained for DPPC-water in a previous work of this group (Morini et al., 2015). It is noticeable that although water is the solvent and DPPC a zwitterionic lipid, with net charge zero, liposomes exhibited surface charge. Accding to those studies, DPPC shown negative values of zeta potential in liquid crystalline state and positive ones in solid crystalline state. In this work, in the presence of XA or XA_1, the mentioned behavior of DPPC is kept, but the mixtures with polyhydroxylated xanthones show negative zeta potentials all over the range of the working temperatures, that is, both in solid crystalline and liquid crystalline state.

For the mixtures DPPC-XA and DPPC-XA_1 it is shown in the graph of temperature dependence of the zeta potential that the phase transition takes place with an abrupt change in the zeta potential values and less sharp change for the DPPC-$XA_{1,3}$ and DPPC-$XA_{1,3,6}$ mixtures. It can also be observed that transition temperatures of the first two systems mentioned are close to that of pure DPPC, while those corresponding to DPPC-$XA_{1,3}$ and DPPC-$XA_{1,3,6}$ mixtures, are significantly smaller than DPPC's.

The transition temperatures were obtained from a rigorous mathematical treatment of the ZP data for each system studied, applying the methodology depicted in Section 2.1.4. Fig. 4a and b shows the adjusted curve and the graph of the curvature function, respectively, for the sample DPPC-XA_1 as an example.

The predicted transition temperature with the proposed methodology has a total error which is the sum of the experimental error and the errors that arise from the different calculations made. The adjustment of the experimental data, in the sense of the minimum squares with a model of harmonic functions, has a deviation given by the norm of the residual vector. The calculation of the transition temperature, solving the equation $f''(T, A_*) = 0$. with Newton's method, has an error of about 0.0001%. These errors are negligible with respect to the experimental one.

Transition temperatures obtained by ZP were corroborated by DSC. Although temperature dependence of the ZP method was presented in our previous study (Sierra et al., 2016), this was applied to lipid mixtures, while in this work the mixtures are composed of a lipid and a dopant. Fig. 5 shows thermograms of the

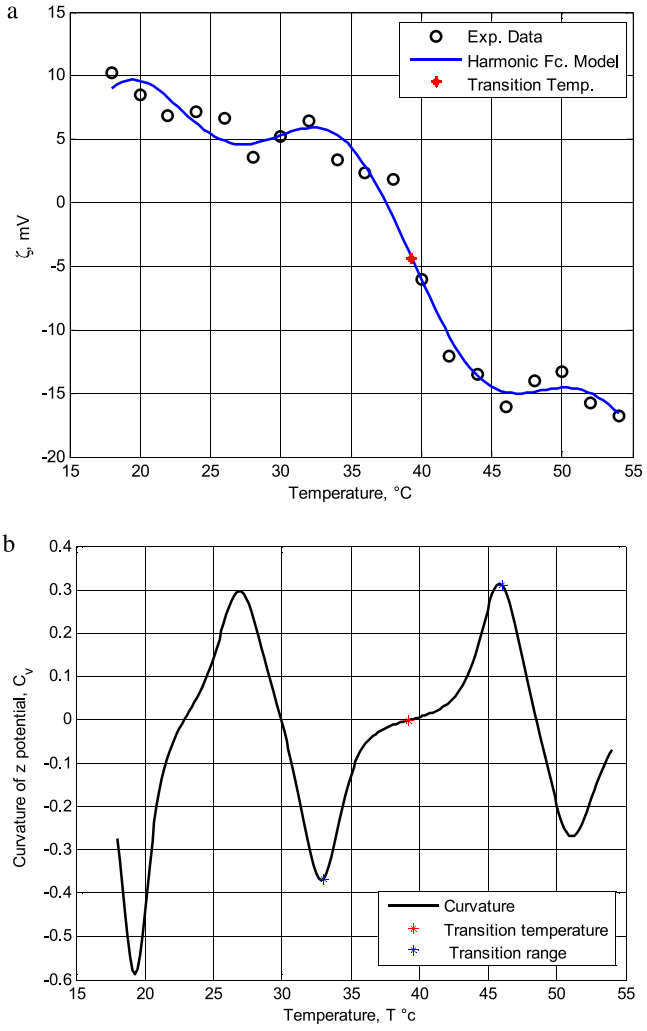

Fig. 4. a Zeta potential as a function of Temperature for DPPC-XA_1. Experimental data (o). Curve estimated by least squares of zeta potential (blue line). Transition temperature (*). b Graph of the curvature function of the model of harmonic functions for DPPC-XA_1, endpoints transition zone (blue *) and transition temperatures (red *). (For interpretation of the references to color in this figure legend, the reader is referred to the web version of this article.)

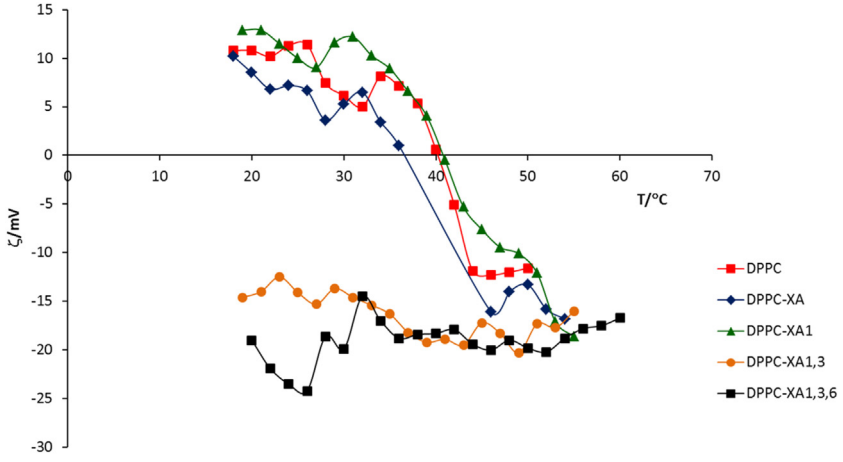

Fig. 3. Zeta potential as a function of T for DPPC and DPPC-XAs, prepared and dispersed in water.

studied samples, superimposed for comparative purposes. It is observed that the DPPC-XAs mixtures present lower transition temperatures than pure DPPC and the transition temperature of those mixtures decreases with the increase of hydroxyl groups in the xanthones. Similar trend is observed in the widening of the peaks with respect to the DPPC without adding XAs. All the results of transition temperatures are collected in Table 1.

Fig. 6 shows the temperature dependence of the conductivity. The conductivity values are slightly higher than those for pure water. DPPC liposomes show the highest conductivity values while the DPPC-$XA_{1,3,6}$ mixture shows the lower ones. In all cases, a smooth variation of conductivity with temperature is observed, with no appreciable changes around the transition temperature of the liposome.

The pH of the different systems did not show significant differences either respect to the solvent or with the temperature. Regarding the size of the liposomes studied, no significant changes were observed as a function of the temperature (data not shown).

We conducted molecular dynamics simulations in order to measure the time evolution of the RMSD of the lipid membrane atoms. We considered only the heavy atoms (that is, all atoms but hydrogen atoms) and subdivided the lipid chains in two groups: the polar part, or lipid head group, and the nonpolar part, that is, the hydrophobic portion of the DPPC molecule. In this study we also focused on lipids that are neighbors of the xanthones molecules. To identify such lipid chains, we used a distance cutoff of 4 Å between any heavy atoms of the xanthones molecules and the lipid chains. RMSD measures the deviation of a target set of atoms from a reference or initial set of coordinates, and is defined as:

$$RMSD = \sqrt{\frac{\sum_{i=0}^{N}\left[m_i(x_i - y_i)^2\right]}{M}}$$

where N is the number of atoms, m_i is the mass of atom i, X_i is the coordinate vector for target atom i, Y_i is the coordinate vector for reference atom i, and M is the total mass.

According to previous considerations made in this work, we have chosen as examples two XAs that affect DPPC properties

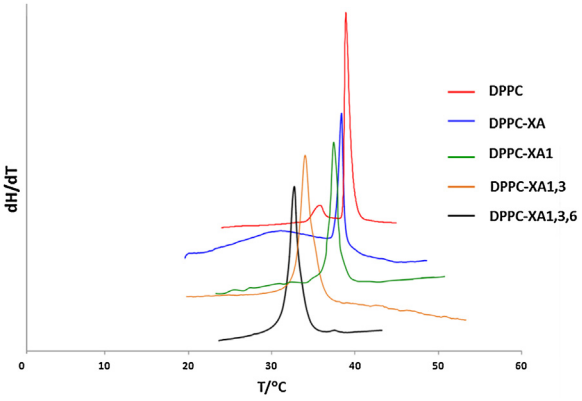

Fig. 5. Waterfall plot of thermograms of the DPPC-XAs mixtures studied. Ordinates axis, dH/dT, in arbitrary units.

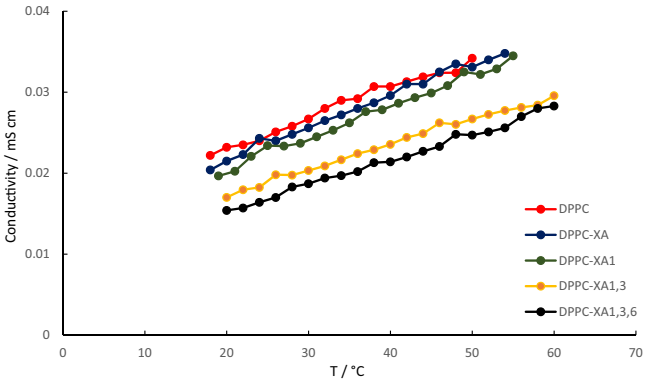

Fig. 6. Temperature dependence of the conductivity of the DPPC-XAs studied mixtures.

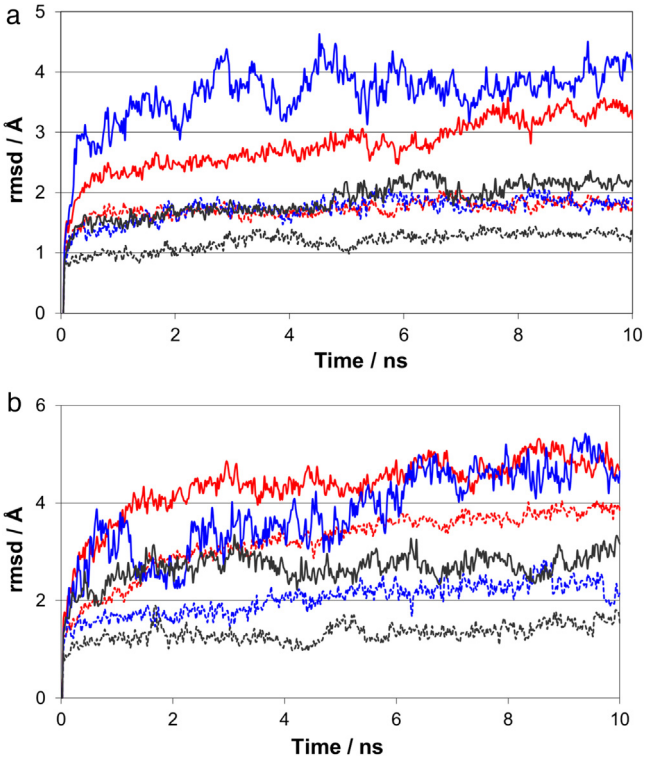

Fig. 7. a Root mean square deviations (rmsd) for gel phase at 20 °C. The results shown correspond to the last 10 ns of the total trajectory.
—— Polar neighbor($XA_{1,3,6}$) —— Polar neighbor(XA_1) —— Polar not neighbor (DPPC)
---- Nonpolar neighbor ($XA_{1,3,6}$) ----- Nonpolar neighbor (XA_1) ----- Nonpolar not neighbor (DPPC).
b Root mean square deviations (rmsd) for fluid phase at 50 °C. The results shown correspond to the last 10 ns of the total trajectory.
—— Polar neighbor($XA_{1,3,6}$) —— Polar neighbor(XA_1) —— Polar not neighbor (DPPC)
---- Nonpolar neighbor ($XA_{1,3,6}$) ----- Nonpolar neighbor (XA_1) ----- Nonpolar not neighbor (DPPC).

Table 1
Transition temperatures and transition range obtained for ZP and Transition temperatures DSC measurements for DPPC and DPPC-XAs mixtures in water. Data are presented as mean ± SD.

System	Range of transition/°C ZP	Ttransition/°C	
		ZP	DSC
DPPC	[35.2, 45.9]	42.4 ± 1.1	41.1 ± 0.8
DPPC-XA	[32.5, 43.9]	38.5 ± 2.0	39.3 ± 1.2
DPPC-XA_1	[30.8, 41.0]	37.5 ± 1.5	38.1 ± 1.0
DPPC-$XA_{1,3}$	[32.0, 39.3]	35.4 ± 0.9	34.9 ± 0.5
DPPC-$XA_{1,3,6}$	[31.9, 37.0]	33.6 ± 1.3	33.2 ± 1.0

differently: XA_1 and $XA_{1,3,6}$. Nine DPPC molecules located at alternate positions in the monolayer were replaced by XA_1 (or $XA_{1,3,6}$). The RMSD of both systems were studied both in gel (Fig. 7a) and fluid state (Fig. 7b). Comparing the time evolution of the RMSD of lipid chains in a pure DPPC membrane with that of xanthone-neighboring lipids in the xanthone-containing membranes, different behaviors were observed: in the gel state the mobility of the headgroup atoms of $XA_{1,3,6}$-neighboring lipids is lower than the mobility of the headgroup atoms of XA_1-neighboring lipids and both higher than that of pure DPPC. In the case of non-polar groups, no appreciable difference was found amongst the different types of xanthones, but the rmsd values were all higher than that of pure DPPC. In the fluid phase, the headgroup atoms near XA_1 and $XA_{1,3,6}$ present similar displacements between them and higher than those lipids that conform a pure DPPC membrane. As for the displacement of nonpolar groups, these are significantly influenced by the presence of the $XA_{1,3,6}$, since these atoms present important movements compared with the same group of atoms neighboring XA_1. In this case, both displacements resulted higher than pure DPPC's.

In summary, the presence of XA_1 and $XA_{1,3,6}$ in the DPPC membrane seems to affect it at the level of the polar groups in gel state and within the non-polar groups in fluid state.

Positions of XA_1 and $XA_{1,3,6}$ were analyzed over time by the different trajectories studied. It was observed that in gel state $XA_{1,3,6}$ oscillated in a lower range of depths compared to XA_1; in fluid phase a similar behavior was observed. This diffusive movement through the membrane occurs until both XAs reach its equilibrium positions. Fig. 8 shows the xanthones averaged distances from the center of the membrane. The distributions of the average distances along the Z axis of all the xanthones of the mixed bilayers show that in fluid phase, $XA_{1,3,6}$ and XA_1, both tend to stay closer to the non-polar groups, while in the gel state, XA_{136} tends to stay closer than XA_1 to the surface. Comparing each xanthone in both states it is observed that in the gel phase the membrane tends to expel the xanthones towards the surface, being this effect more pronounced in $XA_{1,3,6}$ than in XA_1.

4. Discussion

Analyzing structures of the studied xanthones (Fig. 2), taking the skeleton (XA) as a reference, it is clear that XA_1 is in a favorable position for interacting with the xanthone carbonyl by H-bridge. It can be inferred that this hydroxyl group would have low possibilities of interacting with the lipid. In the structures $XA_{1,3}$ and $XA_{1,3,6}$ the 3 and 6 hydroxyl groups are far from the carbonyl, therefore can stablish electrostatic interactions with the positively charged amine groups present in the choline of the polar head region of the phospholipids.

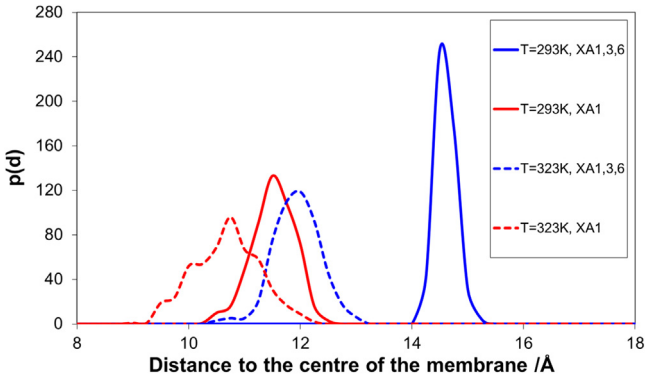

Fig. 8. Distribution of average distances along the Z axis of xanthones in both phases (p(d)).

4.1. Proposal of localization of xanthones

Zeta potential results clearly divide the effect of the molecules studied into two groups: XA_1 and skeleton (XA), which both have similar behavior than DPPC, and polyhydroxylated xanthones, which seem to quite strongly affect surface properties of DPPC. The latter effect, is reflected mainly during the main transition with small zeta potential change (compared to that of XA_1 and XA) and absent change of the sign. Those effects make that both phases resemble on the liposome surface arrangement. In the presence of XA or XA_1 systems exhibit zeta potential negative in fluid and positive in gel, similar to the behavior of DPPC, while the group of polyhydroxylated, show negative potential in both gel and fluid state. Upon our previous work (Morini et al., 2015), the XA and XA_1 would allow the change of conformation of DPPC during the phase change, while polyhydroxylated xanthones prevent, presumably for esteric effect, the change of direction of the polar head group, keeping phosphate group exposed to the surface.

The temperature dependence conductivity data of the different systems reinforce our proposal: firstly, the surface charge would be a consequence of the conformational arrangement of the lipid and not of the dissociation of the polar group originated by the pH of the medium, since in our work the pH remains approximately constant around neutrality throughout the studied temperature range. In addition, the systems show low conductivity, slightly higher than those of water. The behaviour of the conductivity of these systems with the temperature is very different from that presented with the temperature dependence of the potential zeta. Second, the low conductivity values presented by the DPPC-$XA_{1,3}$ and DPPC-$XA_{1,3,6}$ systems would confirm that the negative charge of the DPPC phosphate group, would be compromised in the formation of the intermolecular hydrogen bridge with the corresponding XA, resulting in a minor electrical conduction. According to these results, one possible configuration that may adopt the liposome DPPC-XA_1 is proposed (Fig. 9a). Similar configuration would asume the mixture DPPC-XA as it demostrated similar behaviour. Fig. 9b shows one plausible configuration for the mixture DPPC-$XA_{1,3,6}$. It is noticeable that DPPC-$XA_{1,3,6}$ and DPPC-$XA_{1,3}$ mixtures seem to have the possibility of forming H-bond in gel phase and this would promote that XA molecule remains 'anchorage' to the lipid polar groups, determining preferential exposition of the phosphate group in solid crystalline state.

Fig. 9b shows every possible DPPC-$XA_{1,3,6}$ H-bond and green coloured, that related to the conductivity behaviour.

Besides in this state, the H-bond forming effect is favored by both the closeness of the $XA_{1,3,6}$ to the surface and the temperature of the system. This effect is not observed in the fluid state because of the deeper location of the $XA_{1,3,6}$.

Results obtained from molecular dynamics support this proposal. As it can be observed in Fig. 7, the presence of the $XA_{1,3,6}$ in the gel phase restricts the movement of the polar groups close to the XA molecule. This effect is presumably stronger in XA than in XA_1, because the possibility of H-bond forming between $XA_{1,3,6}$ molecule and the lipid molecules, restricting the movement of the polar groups. In the fluid state, the most appreciable effects are at the level of the non-polar groups of the lipid, indicating this place as a possible location of XAs.

Being clear that an univocal interpretation is difficult, this hypothesis would explain the fact that the presence of xanthones in the membrane causes a stronger effect at the level of the polar groups in the gel phase and in the non-polar groups in the fluid state.

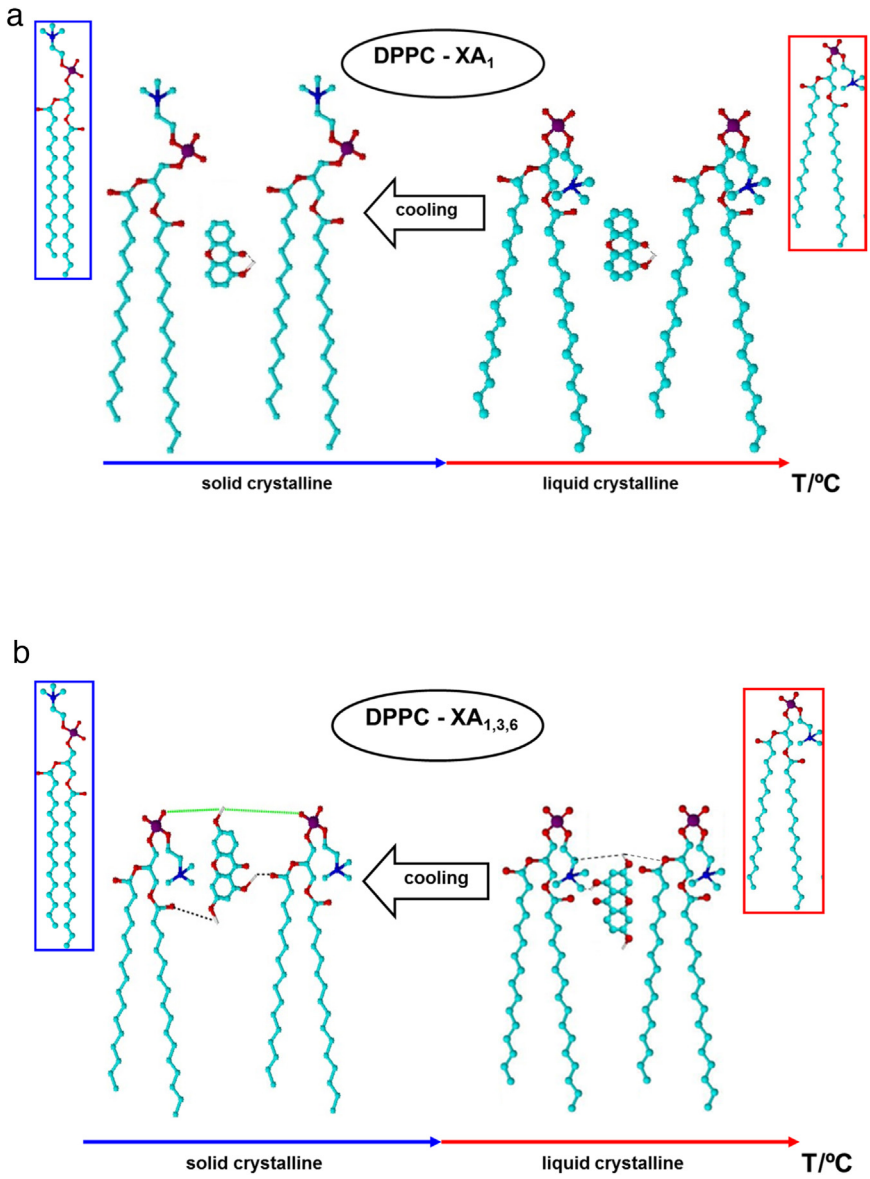

Fig. 9. a Configuration of the proposed structure for DPPC-XA_1. b Configuration of the proposed structure for DPPC-$XA_{1,3,6}$.

4.2. Hydroxy-xanthones effect on membrane fluidity

The results from ZP and DSC measurements showed that in all the DPPC-XAs liposomes, the phase transition temperature of DPPC was shifted to a lower temperature region expressed in Table 1. Solubilization of xanthones made the bilayer membrane heterogeneous and the cooperation of the gel-fluid phase transition was decreased subsequently causing the phase transition to shift to a lower temperature. Particularly, $XA_{1,3}$ and $XA_{1,3,6}$ demonstrated to be perturbing agents which conflict with the interactions between the phospholipids acyl chains. It involves the lowering of $T_{transition}$ (Table 1) also observed in the DSC studies (Fig. 5). Besides, the widening of the peaks of DPPC-XAs respect to pure DPPC reflects that the addition of the dopant disrupts the lipid cooperativity in both phases.

From the point of view of the molecular dynamics, it is observed that the DPPC fluidity at the liquid crystalline phase, is increased with the adding of xanthones, especially the $XA_{1,3,6}$, observed in the higher DPPC hydrocarbon groups displacement (Fig. 7a). Conversely, in the solid crystalline phase, the increase in this mentioned effect is due to the polar heads of DPPC, mainly caused by the presence of XA_1 in the DPPC membrane (Fig. 7b).

In summary, the hydroxylated xanthone responsible for the change of fluidity in the fluid phase is the $XA_{1,3,6}$ while in the gel phase, is the XA_1.

It must be pointed out that experimental studies allowed to analyze fluidity from the transition temperatures while molecular dynamics let investigate fluidity changes within each particular phase state.

5. Conclusion

Zeta potential with continuous cooling, DSC and computational simulation were used in this first study of interactions of hydroxyl-xanthones with phospholipids membranes. This work allowed to analize two features related to this interaccion: by one side, the posible location of the xanthones in the membrane and, by the other side, the fluidizing effect over the membrane, as it have being approached from both the experimental studies and the simulation.

About location, the polyhydroxylated xanthones seem to present relocalization when passing from the fluid phase to the gel phase, while the 'less' hydroxylated ones would remain in the same position.

From the DPPC membrane fluidity point of view, all the studied xanthones increased it. The interesting fact of this work was that polyhydroxylated xanthones presented more fluidizing effect in the fluid phase of the DPPC while with the 'less' hydroxylated ones this effect is more pronounced in the gel phase.

Acknowledgements

Financial support from CONICET, ANPCyT and UNS is gratefully acknowledged. M.B.S, L.A., D.G. and M.A.M., are members of the research career of CONICET. Authors thank Dr. Marcelo Avena for allowing the use of Zetasizer Nano ZS90 equipment.

References

de Koning, C.B., Giles, R.G.F., Engelhardt, L.M., White, A.H., 1988. J. Chem. Soc Perkin Trans. 1 3209 and references therein.

Bothun, G.D., 2008. Hydrophobic silver nanoparticles trapped in lipid bilayers: size distribution, bilayer phase behavior, and optical properties. J. Nanobiotechnol. 6, 13.

Brittes, J., Lúcio, M., Nunes, C., Lima, J.L.F.C., Reis, S., 2010. Effects of resveratrol on membrane biophysical properties: relevance for its pharmacological effects. Chem. Phys. Lipids 163, 747–754.

Chairungsrilerd, N., Furukawa, K., Ohta, T., Nozoe, S., Ohizumi, Y., 1996. Pharmacological properties of alpha-mangostin, a novel histamine H1 receptor antagonist. Eur. J. Pharmacol. 314, 351–356.

Dodean, R.A., Kelly, J.X., Peyton, D., Gard, G.L., Riscoe, M.K., Winter, R.W., 2008. Synthesis and heme-binding correlation with antimalarial activity of 3,6-bis-(ω-N,N-diethylaminoamyloxy)-4,5-difluoroxanthone. Bioorg. Med. Chem. 16, 1174–1183.

El-Seedi, H.R., El-Barbary, M.A., El-Ghorab, D.M.H., Bohlin, L., Borg-Karlson, A.-K., Goransson, U., Verpoorte, R., 2010. Recent insights into the biosynthesis and biological activities of natural xanthones. Curr. Med. Chem. 17, 854–901.

Goncalves Azevedo, C.M., Magalhaes Afonso, C.M., Magalhaes Pinto, M.M., 2012. Routes to xanthones: an update on the synthetic approaches. Curr. Org. Chem. 16, 2818–2867.

Hauser, H., Pascher, I., Pearson, R.H., Sundell, S., 1981. Preferred conformation and molecular packing of phosphatidylethanolamine and phosphatidylcholine. Biochim. Biophys. Acta 650, 21–51.

Iinuma, M., Ito, T., Miyake, R., Tosa, H., Tanaka, T., Chelladurai, V., 1998. A xanthone from Garcinia cambogia. Phytochemistry 47, 1169–1170.

Koh, J.-J., Lin, S., Aung, T.T., Lim, F., Zou, H., Bai, Y., Li, J., Lin, H., Pang, L.M., Koh, W.L., Salleh, S.M., Lakshminarayanan, R., Zhou, L., Qiu, S., Pervushin, K., Verma, C., Tan, D.T.H., Cao, D., Liu, S., Beuerman, R.W., 2015. Amino acid modified xanthone derivatives: novel, highly promising membrane-active antimicrobials for multidrug-resistant gram-positive bacterial infections. J. Med. Chem. 58, 739–752.

Kolokythas, G., Kostakis, I.K., Pouli, N., Marakos, P., Skaltsounis, A.-L., Pratsinis, H., 2002. Design and synthesis of some new pyranoxanthenone aminoderivatives with cytotoxic activity. Bioorg. Med. Chem. Lett. 12, 1443–1446.

Lasic, D.D., 1997. Liposomes in Gene Delivery. CRC Press.

Lin, C.N., Liou, S.J., Lee, T.H., Chuang, Y.C., Won, S.J., 1996. Xanthone derivatives as potential anti-cancer drugs. J. Pharm. Pharmacol. 48, 539–544.

Mabrey, S., Sturtevant, J.M., 1976. Investigation of phase transitions of lipids and lipid mixtures by sensitivity differential scanning calorimetry. Proc. Natl. Acad. Sci. 73, 3862–3866.

Matsumoto, K., Akao, Y., Kobayashi, E., Ohguchi, K., Ito, T., Tanaka, T., Iinuma, M., Nozawa, Y., 2003. Induction of apoptosis by xanthones from mangosteen in human leukemia cell lines. J. Nat. Prod. 66, 1124–1127.

Matsumoto, K., Akao, Y., Yi, H., Ohguchi, K., Ito, T., Tanaka, T., Kobayashi, E., Iinuma, M., Nozawa, Y., 2004. Preferential target is mitochondria in alpha-mangostin-induced apoptosis in human leukemia HL60 cells. Bioorg. Med. Chem. 12, 5799–5806.

Menéndez, C.A., Nador, F., Radivoy, G., Gerbino, D.C., 2014. One-step synthesis of xanthones catalyzed by a highly efficient copper-based magnetically recoverable nanocatalyst. Org. Lett. 16, 2846–2849.

Morini, M.A., Sierra, M.B., Pedroni, V.I., Alarcon, L.M., Appignanesi, G.A., Disalvo, E.A., 2015. Influence of temperature, anions and size distribution on the zeta potential of DMPC, DPPC and DMPE lipid vesicles. Colloids Surf. B: Biointerfaces 131, 54–58.

Onuki, Y., Hagiwara, C., Sugibayashi, K., Takayama, K., 2008. Specific effect of polyunsaturated fatty acids on the cholesterol-poor membrane domain in a model membrane. Chem. Pharm. Bull. 1103–1109.

Park, S.-H., Oh, S.-G., Mun, J.-Y., Han, S.-S., 2005. Effects of silver nanoparticles on the fluidity of bilayer in phospholipid liposome. Colloids Surf. B: Biointerfaces 44, 117–122.

Park, S.-H., Oh, S.-G., Mun, J.-Y., Han, S.-S., 2006. Loading of gold nanoparticles inside the DPPC bilayers of liposome and their effects on membrane fluidities. Colloids Surf. B: Biointerfaces 48, 112–118.

Pinto, M.M.M., Sousa, M.E., Nascimento, M.S.J., 2005. Xanthone derivatives: new insights in biological activities. Curr. Med. Chem. 12, 2517–2538.

Rodríguez-Pulido, A., Ortega, F., Llorca, O., Aicart, E., Junquera, E., 2008a. A physicochemical characterization of the interaction between DC-Chol/DOPE cationic liposomes and DNA. J. Phys. Chem. B 112, 12555–12565.

Rodríguez-Pulido, A., Aicart, E., Llorca, O., Junquera, E., 2008b. Compaction process of calf thymus DNA by mixed cationic-zwitterionic liposomes: a physicochemical study. J. Phys. Chem. B 112, 2187–2197.

Rodríguez-Pulido, A., Martín-Molina, A., Rodríguez-Beas, C., Llorca, O., Aicart, E., Junquera, E., 2009. A theoretical and experimental approach to the compaction process of DNA by dioctadecyldimethylammonium bromide/zwitterionic mixed liposomes. J. Phys. Chem. B 113, 15648–15661.

Sierra, M.B., Pedroni, V.I., Buffo, F.E., Disalvo, E.A., Morini, M.A., 2016. The use of zeta potential as a tool to study phase transitions in binary phosphatidylcholines mixtures. Colloids Surf. B: Biointerfaces 142, 199–206.

Skjevik, Å.A., Madej, B.D., Walker, R.C., Teigen, K., 2012. LIPID11: a modular framework for lipid simulations using amber. J. Phys. Chem. B 116, 11124–11136.

Sulkowski, W.W., Pentak, D., Nowak, K., Sulkowska, A., 2005. The influence of temperature, cholesterol content and pH on liposome stability. J. Mol. Struct. 744–747, 737–747.

Tatulian, S.A., 1983. Effect of lipid phase transition on the binding of anions to dimyristoylphosphatidylcholine liposomes. Biochim. Biophys. Acta 736, 189–195.

Tieleman, D.P., Marrink, S.J., Berendsen, H.J.C., 1997. A computer perspective of membranes: molecular dynamics studies of lipid bilayer systems. Biochim. Biophys. Acta 1331, 235–270.

Tocci, N., Simonetti, G., D'Auria, F.D., Panella, S., Palamara, A.T., Valletta, A., Pasqua, G., 2011. Root cultures of Hypericum perforatum subsp angustifolium elicited with chitosan and production of xanthone-rich extracts with antifungal activity. Appl. Microbiol. Biotechnol. 91, 977–987.

Villarreal, M.A., Perduca, M., Monaco, H.L., Montich, G.G., 2008. Binding and interactions of L-BABP to lipid membranes studied by molecular dynamic simulations. Biochim. Biophys. Acta 1778, 1390–1397.

Wang, Y., Xia, Z., Xu, J.-R., Wang, Y.-X., Hou, L.-N., Qiu, Y., Chen, H.-Z., 2012. α-Mangostin, a polyphenolic xanthone derivative from mangosteen, attenuates β-amyloid oligomers-induced neurotoxicity by inhibiting amyloid aggregation. Neuropharmacology 62, 871–881.

Wang, S., Li, Q., Jing, M., Alba, E., Yang, X., Sabaté, R., Han, Y., Pi, R., Lan, W., Yang, X., Chen, J., 2016. Natural xanthones from garcinia mangostana with multifunctional activities for the therapy of Alzheimer's disease. Neurochem. Res. 41, 1806–1817.